New Ideas and Tools for Designing Optimized Stellarator Coils

Prashant Valanju, William Miner

Fusion Research Center, University of Texas at Austin

Art Brooks, Neil Pomphrey

Princeton Plasma Physics Laboratory

Steven Hirshman, Lee Berry

Oak Ridge National Laboratory

We present new ideas and a complete collection of tools for solving the difficult problem of designing, under various physics and engineering constraints, optimized coils for low aspect ratio stellarators. These include various upgrades to enhance the abilities of the NESCOIL code to obtain a surface current distribution which reproduces the desired plasma shape. We have also added the capability to target, within NESCOIL, the resonant errors produced by the current sheet. For the next design step of obtaining filamentary coils from the surface currents, we present a novel use of the genetic algorithm which improves and hastens the search for a deep minimum in the optimization criteria within a very large parameter space. For the final design step of obtaining finite-size coils from the filaments, we present a series of ideas and codes to allow efficient targeting of various engineering constraints. Taken together, this suite of codes has enabled us to successfully design saddle coils for the optimized quasi-axisymmetric (QA) plasma under consideration for the National Compact Stellarator Experiment (NCSX) and modular coils for the quasi-omnigenous (QO) configuration.

1 Introduction

The relatively recent discoveries of compact (low aspect ratio) stellarators that are optimized to improve various physical properties have opened up new and exciting branches of stellarator research. The general trend in designing the new configurations is towards partially restoring some symmetry that would be otherwise lost at low aspect ratios. The Quasi-Axisymmetric (QA)[2] and Quasi-Omnigeneous (QO)[3] stellarators are two leading examples of such optimized configurations which can have very good orbit, transport, and stability properties.

Nature, however, extracts a price for this improvement in the form of generally increased difficulty in designing suitable coils to produce these optimized configurations. We faced this hardship when we started designing coils for a QA National Compact Stellarator Experiment (NCSX)[5] for Princeton Plasma Physics Laboratory (PPPL) and a QO concept exploration (CE)[6] experiment. Using the Neumann Equation Solver code NESCOIL[1] we could not complete even the first step of obtaining a surface current distribution from which realistic discrete coils could be cut to create the plasma configurations. The current distributions required for an acceptable plasma reconstruction (as defined by plasma properties such as good surfaces, stability, quasi-symmetry, etc.) were too complex for realistic coils and there was no systematic way of smoothing them within NESCOIL. There was also no way of systematically reducing the current density and the resonant errors created on the plasma surface. Similar difficulties for QO configurations indicated that they may be generic to these optimized, compact configurations, and that a better method was needed to overcome them.

We have solved these problems without abandoning the linear Green's function method which is faster than non-linear optimizers. We have written, tested, and successfully used for QA and QO an enhanced Green's function code NESVD. In it we replace the least-square solver in NESCOIL by a Singular Value Decomposition (SVD) technique[4]. This method allows us to obtain an ordered set of progressively smoother "natural" current distributions by varying the number of svd weights retained. An optimum solution can then be chosen from this set to minimize any one of many targets (such as the surface current density) while the plasma reconstruction stays within acceptable limits set by desired physical properties. We have also implemented a linear modification of the NESCOIL Green's functions for the minimization of resonant field errors within this SVD method. These new capabilities along with the high speed of NESVD have enabled us to successfully tackle the task of exploring many new QA and QO plasma configurations with good coil design feasibility and creating initial coil designs

which can be further engineered into realistic coils.

In the next section we describe the new NESVD code and describe a method of using NESVD which has proved successful in actual coil designs. In Sec.3 we present NESVD results for some QA and QO configurations which were not amenable to an attack with NESCOIL.

2 NESVD: Enhanced NESCOIL code

2.1 A brief review of NESCOIL[1]

NESCOIL solves the exterior Neumann problem of finding a current distribution $j(u,v)$ on a fixed, plasma-enclosing "coil winding surface" (CWS) which minimizes the normal component of the total magnetic field $B(u',v')$ on the plasma surface (PLS) (see Fig.1). For this it uses the Green's function method described in Ref.[1]. Here we give a quick summary of NESCOIL before explaining our modifications.

In this paper toroidal surfaces with N field periods will be mapped into poloidal ($0 \le u < 1$) and toroidal ($0 \le v < N$) coordinates, with (u,v) and (u',v') denoting the current and plasma surfaces (CWS and PLS) respectively. The current distribution at (u,v) on the CWS is given via the surface gradient of the scalar current potential function $\phi(u,v)$

$$\bar{j}(u,v) = \hat{n} \times \nabla\phi(u,v), \tag{1}$$

where $\hat{n}$ is the outward normal to the CWS and $\phi(u,v)$ can be written in terms of MF poloidal and NF toroidal fourier modes by

$$\phi(u,v) = \sum_{m=0}^{MF} \sum_{n=-NF}^{NF} \phi(m,n) \sin(2\pi[mu+nv]) - \frac{I_p}{N} v - I_t u. \tag{2}$$

The secular terms I_p and I_t are the net poloidal and toroidal currents on the CWS. A direct application of Biot-Savart law allows one to express the normal component $B_\perp$ of the total magnetic field $\bar{B}(u',v')$ produced at a point (u',v') on PLS by the surface current $\bar{j}(u,v)$ on CWS in the form of a linear equation in $\phi(m,n)$ and the Green's functions $H(u',v')$ and $G(u',v'|m,n)$ (see Ref.[1])

$$B_\perp(u',v') = H(u',v') + \sum_{m=0,n=-NF}^{MF,NF} G(u',v'|m,n)\phi(m,n) = -B_{\perp,ext}, \tag{3}$$

where $H(u',v')$ comes from the "constant" term I_p. The task is to minimize $B_{err} \equiv (B_\perp + B_{\perp,ext})$, i.e., to find $\phi(m,n)$ for which the $B_\perp$ created by the surface currents cancels the $B_{\perp,ext}$ created by the plasma current and any other fixed external coils (such as toroidal and vertical field coils). The linear equation 3 is solved in NESCOIL by using the least-squares method where

$$\chi^2 \equiv \int_{PLS} ds' B_{err}^2 = \sum_{u',v'}^{NU',NV'} ds' (B_\perp + B_{\perp,ext})^2 \tag{4}$$

is minimized by varying $\phi(m,n)$. Here the integral is written as a sum over (NU', NV') grid points on the plasma surface and ds' is the surface area element of that grid point. Differentiating χ^2 with respect to the independent variables $\phi(m,n)$ leads to a linear matrix equation which is solved for $\phi(m,n)$. The contours of constant $\phi(u,v)$ define the filamentary coils corresponding to the current potential (see Fig.2). After finding $\phi(m,n)$ all dependent quantities such as the surface current density, coil curvature etc. can be directly calculated from it.

2.2 Singular Value Decomposition (SVD) Method[4] used in NESVD

The least-square method used in NESCOIL is not the preferred method for solving linear problems like Eq.3 because it is neither flexible nor robust[4]. It is inflexible because the only freedom in trying to reduce the error is changing the number of fourier modes used. The accuracy of a solution in NESCOIL can be increased by using more fourier modes, but this also increases coil complexity (see Fig.2), and there is no way within NESCOIL to disentangle the two effects. It is also not robust because it often fails when many combinations of the modes are in the "null space", i.e., many of the modes are not essential for reducing the errors. Only certain "natural" combinations of the modes reduce the error significantly while other combinations have relatively little effect, but the least-square NESCOIL does not provide a way to extract only the "natural" combinations. This redundancy of modes suggests that there may be a better way to solve this problem.

The preferred way of solving Eq.3 is the Singular Value Decomposition (SVD) method where one directly inverts it by decomposing the matrix G into a product of 3 matrices U, w, and V (see [4])

$$G(NUV'|MNF) = U(NUV'|MNF) \cdot w(MNF|MNF) \cdot V(MNF|MNF) \tag{5}$$

where MNF is the total number of fourier modes ($0 \leq m \leq MF$ and $-NF \leq n \leq NF$), NUV' is the total number of grid points on the PLS ($1 \leq iu' \leq NU'$ and $1 \leq iv' \leq NV'$), U is a column-orthogonal matrix, w is a diagonal matrix of MNF non-negative svd weights ordered in decreasing magnitude, and V contains the corresponding MNF svd basis vectors in its columns. The solution of the linear problem is then given by a linear superposition of the weighted svd basis vectors

$$\phi(m,n) = -\sum_{i=1}^{MNF} \left(\frac{U_i \cdot B_{\perp,ext}(u',v')}{w_i} \right) V_i(m,n) \tag{6}$$

Coefficients of each basis vector correspond to one set of fourier components $\phi(m,n)$. The basis vectors V_i with the largest svd weights w_i contribute most to reducing the residual error χ^2. The svd decomposition provides a set of basis vectors which are ordered by their importance in reducing the error. The vectors with zero or small weights are combinations of fourier components that are essentially irrelevant for reducing the error, and can simply be dropped to create smoother solutions without significantly increasing χ^2. This offers a systematic way of smoothing the current contours while still keeping the field errors at nonzero but acceptably low values (see Fig.2). This method is also robust, i.e., it always yields the best possible solution even when the least-square NESCOIL method fails numerically due to the existence of a null-space (some weights are zero), or can give large "probable error" due to a "near-null" space (some weights are nearly zero). It is also flexible because it allows the quick exploration of various tradeoffs, e.g., between accuracy and current density. Finally, it is relatively easy to implement within the existing NESCOIL code and runs just as fast as the least-squares NESCOIL.

A very productive way to use the smoothing information given by the svd decomposition is to use a large number of fourier modes, perform the one necessary svd decomposition in Eq.5, and then calculate an "svd sequence" of solutions by partially summing Eq.6 up to the number of desired svd weights $nsvd$. Each step in this "svd scan" procedure requires one fast matrix multiplication. For each solution one can then quickly calculate various minimization targets such as B_{err}, the maximum current density J_{max}, or the maximum curvature of current lines. Since these quantities do not vary monotonically with $nsvd$, a plot quickly indicates the optimum number of weights to keep. This can be seen in Fig.3 where a local minimum in J_{max} is seen at 121 out of 144 svd weights. Such "svd scans" often yield the smoothness normally obtained by using a small number of fourier modes along with small errors normally obtained by using large number of fourier modes. These local minima in svd number space are quite robust, i.e., the preferred number of svd weights changes quite smoothly as the

parameters of the problem are varied. This rapid svd scan technique has proved very effective in designing coils for NCSX-QA and QO. It has produced configurations with lower maximum current density while keeping the error below acceptable levels.

2.3 Linear NESVD Modifications to Control Resonant Field Errors

Although the procedures described so far minimize B_{err} on the outermost plasma surface, they can also be used to minimize any linear function of B_{err}. If the mode structure in the residual B_{err} resonates with the winding number (ι) on the plasma surface, even small amounts of B_{err} could create large displacements X_{err} of the field lines from the surface, i.e, islands and stochastic regions. It is desirable to have the capability of reducing such resonant errors within the above fast procedure because it can then be integrated in the initial scoping studies for good plasma-coil combinations.

For regions with small islands, an approximate procedure for turning the normal error $B_\perp$ into field line displacement X_{err} involves solving the linearized equation:

$$B \cdot \nabla X_{err} = (B^\theta \partial_\theta + B^\phi \partial_\phi) X_{err}(\theta, \phi) = B_\perp |\nabla \rho| \tag{7}$$

on the outermost plasma surface. Here ρ, θ and ϕ are the radial, poloidal, and toroidal coordinate. This equation can be solved by using the functions $\lambda(\theta, \phi)$ (see Ref.[7]) to transform from the (θ, ϕ) coordinates to the straight magnetic field line coordinates (u, v) given by

$$u = \theta + \lambda(\theta, \phi), v = \phi \tag{8}$$

In the (u, v) system, the normal field line displacement $X_{err}(u, v)$ satisfies

$$(\iota \partial_u + \partial_v) X_{err}(u, v) = \frac{B_\perp \sqrt{g} \nabla \rho}{\Phi'(1 + \lambda_\theta)} \equiv b(u, v) \tag{9}$$

where $\sqrt{g}$ and Φ' are the Jacobian and the gradient of the toroidal flux respectively. These quantities are available from the output of the VMEC code[7] which is used to generate the plasma equilibrium. The (u, v) derivatives reduce to multiplication by the mode numbers in the straight-line coordinates and we get the fourier coefficients

of X_{err}

$$\begin{aligned} X_{err}(m,n) &= -\frac{b(m,n)}{m\cdot\iota+n} \\ b(m,n) &= \frac{1}{4\pi^2}\int\int dudv\,\sin(mu+nv)b(u,v) \\ &= \frac{1}{4\pi^2}\int\int \frac{dA}{\Phi'}\sin(m[\theta+\lambda(\theta,\phi)]+n\phi)B_\perp(\theta,\phi) \end{aligned} \tag{10}$$

Since $b(m,n)$ is linear in $\phi(m,n)$, and since its conversion to $X(m,n)$ outlined above is also a linear operation, we can transform the NESCOIL Green's functions H and G of Eq.3 to new Green's functions H_x and G_x to write $X_{err}(m,n)$ as

$$X_{err}(m,n) = H_x(m,n) + \sum_{m'=0,n'=-NF}^{MF,NF} G_x(m,n|m',n')\phi(m',n'), \tag{11}$$

where the modified Green's functions are given in terms of the original functions by

$$\begin{aligned} G_x(m,n|m',n') &= \frac{1}{4\pi^2(m\cdot\iota+n)}\int\int\frac{dA}{\Phi'}\sin(m[\theta+\lambda]+n\phi)G(\theta,\phi|m',n') \\ H_x(m,n) &= \frac{1}{4\pi^2(m\cdot\iota+n)}\int\int\frac{dA}{\Phi'}\sin(m[\theta+\lambda]+n\phi)H(\theta,\phi) \end{aligned} \tag{12}$$

After using Eq.12 to convert H and G to H_x and G_x, the linear Eq.11 can be solved (to make $X_{err}\approx 0$) with the direct svd inversion method discussed in Sec. 2.2. An "svd scan" can then be used to pick out a local nsvd minimum in B_{err} or J_{max} where X_{err} is also small. Coils designed with this procedure are close to those designed to minimize B_{err}, but they show some small wiggles which are critical for reducing X_{err} (see Fig.6). Applications to QA and QO have shown that these small changes are often important in getting a good plasma reconstruction.

3 Applications of NESVD to QA and QO configurations

NESVD has been used as a starting point for designing coils for many QA and QO configurations. These configurations arise as a result of the continuing effort to achieve plasmas with better physical properties. The

task of the NESVD code is to quickly assess the feasibility of designing realistic coils for each new configuration. The results of NESVD become the starting point for a) cutting a small number of filamentary coils from the NESVD surface current solution, b) further refining the coil selection by using the genetic algorithm[8], c) using the COILOPT code[9] to further optimize this coil set by moving the current-carrying surface, and finally d) passing the coil set to the engineering team for detailed design. This procedure is described in detail in Ref.[10].

Case	Method	MF, NF, type	$nsvd$	$B_{err}\%$	J_{max}	$Cmplx$
QA-C10-Sad	NESCOIL	$8, 8$	-	No	Solution	-
	NESCOIL	$20, 20$	-	No	Solution	-
	NESVD	$20, 20$	200	0.14	1.2	2.1
QA-C82-Sad	NESCOIL	$10, 10$	-	0.22	1.17	3.24
	NESVD	$8, 8$	121	0.60	0.83	3.11
	NESVD	$10, 10$	194	0.22	0.94	3.13
	NESVD	$20, 20$	286	0.22	1.38	3.94
	NESVD	$32, 32$	300	0.19	1.35	4.53
QA-Li383-Mod	NESCOIL	$8, 8$	-	0.4	1.0	2.1
	NESCOIL	$20, 20$	-	0.4	1.0	2.1
	NESVD	$8, 8$	121	0.5	0.6	1.8
	NESVD	$20, 20$	286	0.22	1.38	3.94
QO-2fp-Mod	NESCOIL	$8, 8$	-	0.4	1.0	2.1
	NESCOIL	$20, 20$	-	0.4	1.0	2.1
	NESVD	$8, 8$	121	0.5	0.6	1.8
	NESVD	$20, 20$	286	0.22	1.38	3.94
QO-3fp-Mod	NESCOIL	$8, 8$	-	0.4	1.0	2.1
	NESCOIL	$20, 20$	-	0.4	1.0	2.1
	NESVD	$8, 8$	121	0.5	0.6	1.8
	NESVD	$20, 20$	286	0.22	1.38	3.94

Table 1: NESVD and NESCOIL results for QA and QO. The "Sad" and "Mod" refer to saddle and modular coils respectively. Note that a) NESVD gets solutions when NESCOIL cannot (QA-C10), b) NESVD solutions yield lower J_{max} and complexity as well as good B_{err} (QA-C82). c) NESVD advantage pesists for all QA and QO cases.

The results of NESVD and NESCOIL calculations for some QA and QO cases are summarized in Table.(1). For each configuration the number (mf, nf) of fourier modes used, the optimum number $(nsvd)$ of svd weights used in NESVD, the residual B_{err}, the maximum current density (J_{max}), and the complexity of the current contours $(Cmplx \equiv \sum_m m^2\phi(m,n)/\sum_m m\phi(m,n))$ are shown. The NESVD code generally yields smoother

current contours with smaller J_{max} than NESCOIL solutions. It also gets solutions in cases where NESCOIL fails, and allows exploration of tradeoffs between competing goals such as the reduction of B_{err} or J_{max} or X_{err}. Since NESVD does all this with a speed very close to NESCOIL, it is suitable for configuration scoping and optimization tasks.

We show in Fig.1 one of the QA configurations along with a surface on which both NESCOIL and NESVD calculations were performed. The resulting current contours are shown in Fig.2. For this case, the contours required to keep B_{err} below 0.5% are too complex for further coil design. Increasing the number of modes MNF in NESCOIL to reduce B_{err} further increases the complexity. For the same case, NESVD can rescue the situation as shown in Fig.2. This is done by increasing MNF but keeping only a small number (200 out of 861) svd weights. This is possible because NESVD can pick out the "natural" current distributions out of all possible ones, while NESCOIL is forced to use all of them. A careful choice of the number of svd weights kept often allows a smooth solution while also keeping the various errors within acceptable limits.

An example of the tradeoffs involved in choosing the right number of svd weights to keep ($nsvd$) is given in another NESVD scan shown in Fig.3. Such scans are useful in picking out local minima such as the one in J_{max} at $nsvd = 187$ out of 861. We expect only the targeted B_{err} to be monotonic with $nsvd$, and it is seen to drop quickly for $nsvd > 184$. Thus a NESVD scan lets us pick out just the right contours with small J_{max} as well as small B_{err}. The resulting current contours are smoother than the NESCOIL contours, and can be used for further coil design. This NESVD flexibility greatly enhaces the chances of a successful coil design.

Case	Target	MF, NF	$nsvd$	X_{err}%	B_{err}%	$Cmplx$
QA-Li383	B_{err}	8, 8	126	14.4	0.44	2.1
	X_{err}	8, 8	126	2.1	0.57	2.2
Ratio	between	X and B	cases	7.0	1.3	1.05
QA-C10	X_{err}	8, 8	118	0.11	0.8	2.77
	B_{err}	8, 8	126	3.63	0.5	2.35
Ratio	between	X and B	cases	32.2	1.63	1.18

Table 2: X_{err} vs B_{err} targeted XNESVD results for QA and QO. The ratios indicate differeces in targeting X_{err} abd B_{err} for the same case. It is seen that X_{err} can be suppressed by large factors while B_{err}, J_{max}, and $Cmplx$ increase only marginally. This suppression ratio is retained when a finite number of coils are cut from the NESVD solution.

Finally, we show in Table 2 and Figs.4, 5, and 6 the results of targeting the resonant field line displacement

(X_{err}) instead of the residual normal B field (B_{err}). It can be seen that a dramatic reduction of X_{err} (by a factor of 30 in this case) is achieved while the B_{err} still remains low. This improvement possibly depends on the value of the rotational transform near the plasma surface, i.e, the proximity of a rational surface to the outermost plasma surface as defined by VMEC[7]. In the few expensive PIES[12] code runs we have performed for coils designed from X_{err} targeted NESVD runs, we have found good correlation between the reduction of resonant errors and plasma reconstructability (see Figs.4, and 5).

Since the X_{err} targeting in NESVD is implemented within the svd scan capability, all the tradeoff methods discussed above can be applied to designing coils which create small islands. We show an example of this in Fig.7 where we picked $nsvd = 113$ based on low J_{max}. The X_{err} targeting within NESVD reduces the X_{err} by a factor of 7 compared to B_{err} targeting in this case. We then checked whether this gain of 7 in X_{err} survives the process of cutting finite numbers (from 8 to 20 per period) of coils carrying equal currents from this solution. Fig.7 shows that both X_{err} and B_{err} rise by only a factor of 3 even for as few as 6 coils per period, thus staying below the B_{err} targeted sheet current case. We then further lowered the error by applying the genetic algorithm (GA) to this case. This algorithm chooses a set number of coils from all possible current contours and also optimizes the current in each coil by using an svd technique (see Ref.[8] for details). In this case GA gave a good solution with X_{err} just 26% above the sheet current solution with only 8 coils per period.

4 Conclusions

In summary, we have developed and successfully used a new code NESVD which greatly enhances the capabilities of the popular code NESCOIL. The new capabilities include a syatematic and robust method of smoothing the coils, a fast method to control coil-generated resonant field errors, and a very useful technique to rapidly scan many solutions to pick out ones that optimize many coil properties. Our experience shows that NESVD is a useful and essential new tool for the design of compact stellarator coils for which NESCOIL is often inadequate. Its speed also enables the fast assessment of the existence of realistic coils for the many new compact stellarator plasma configurations that are currently being developed. It has been developed in a multi-university collaboration for the National Compact Stellarator coil design task, and is a new resource available to the U.S. stellarator community. Please contact pvalanju@mail.utexas.edu for further details of the code.

Plasma Surface QA-li383
Coil Winding Surface d1826

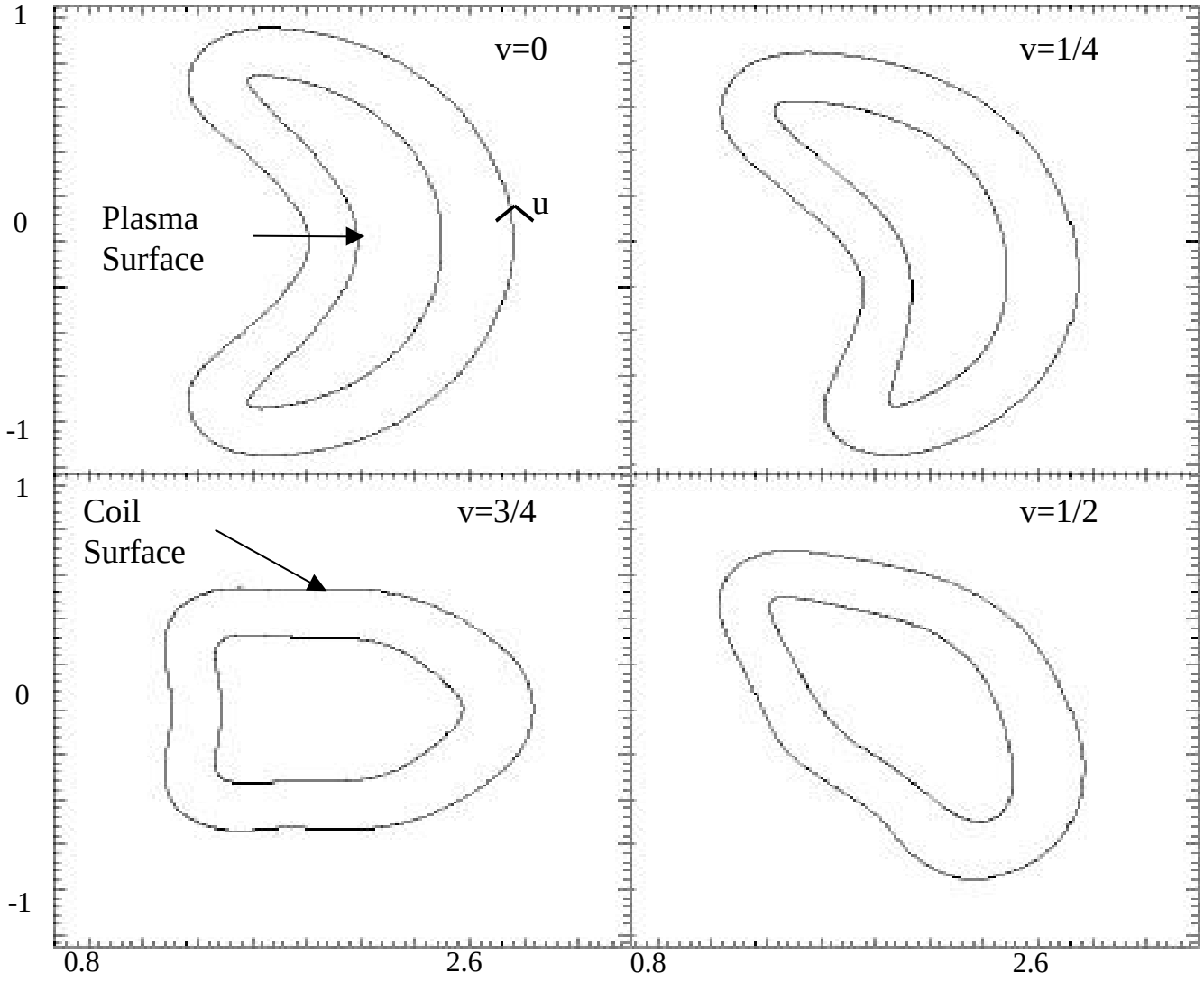

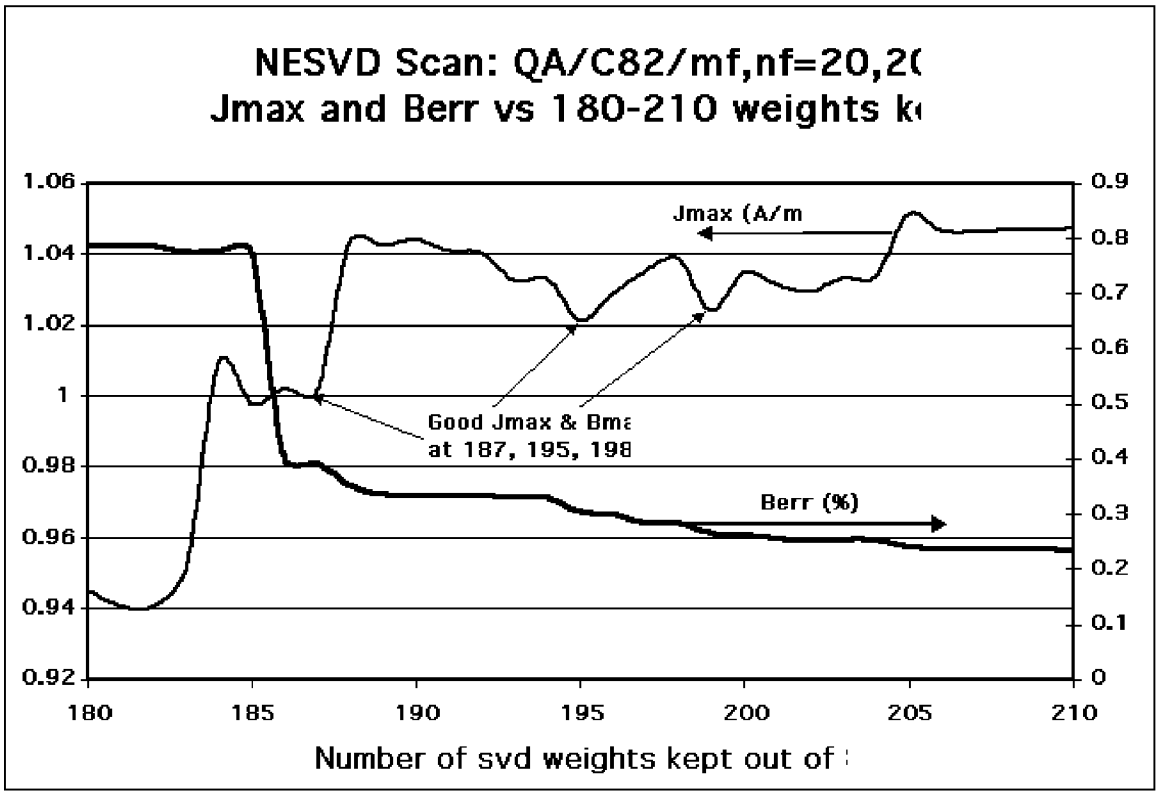

Figure 3: An svd scan for the QA C82 configuration to find the $nsvd$ at which there are local minima of J_{max}. The maximum number of independent fourier modes was 861 for $mf = 20$, $nf = 20$. At $nsvd = 187$ we get good J_{max} as well as B_{err}.

Li 383 Berr vs Xerr Targeted Coils

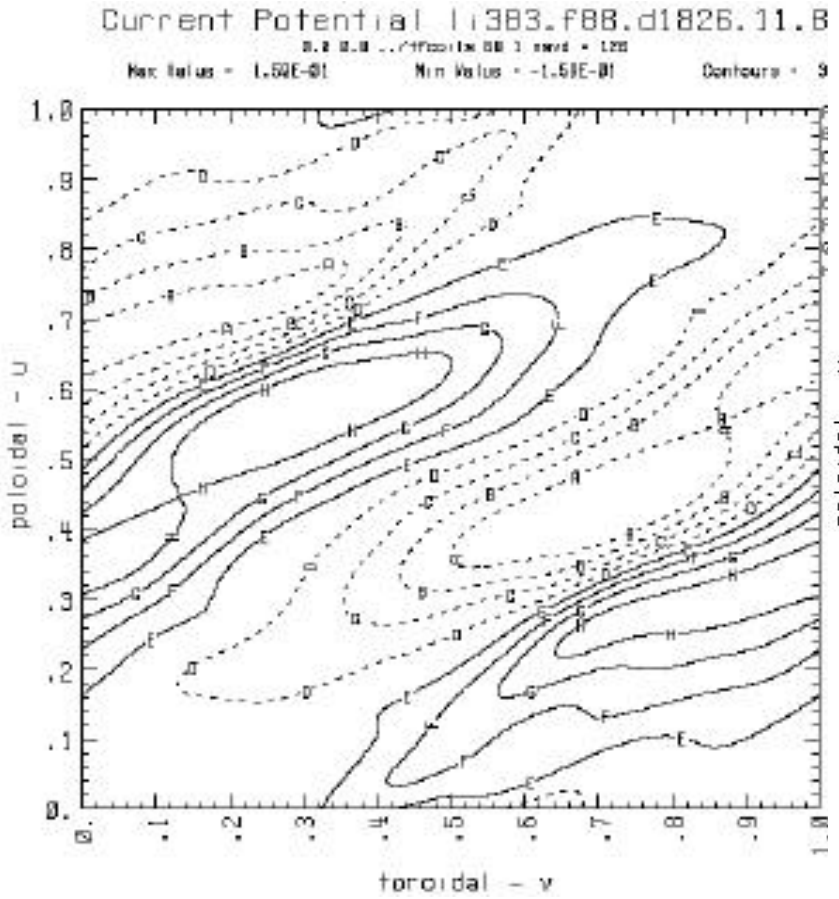

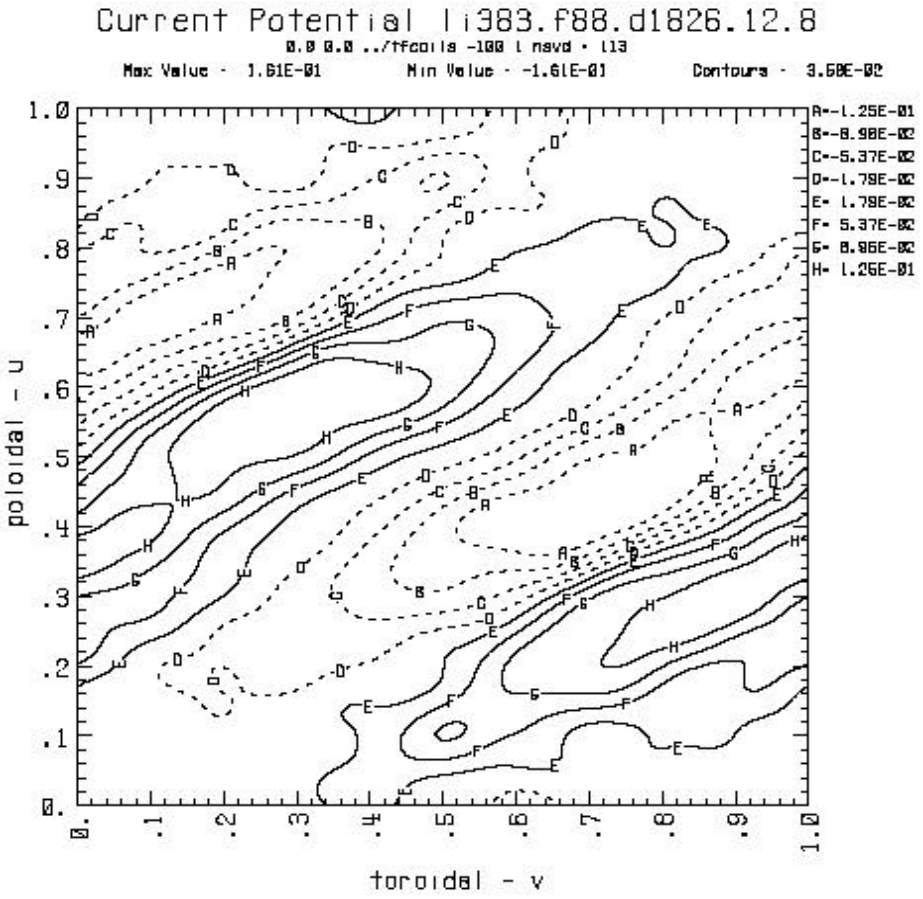

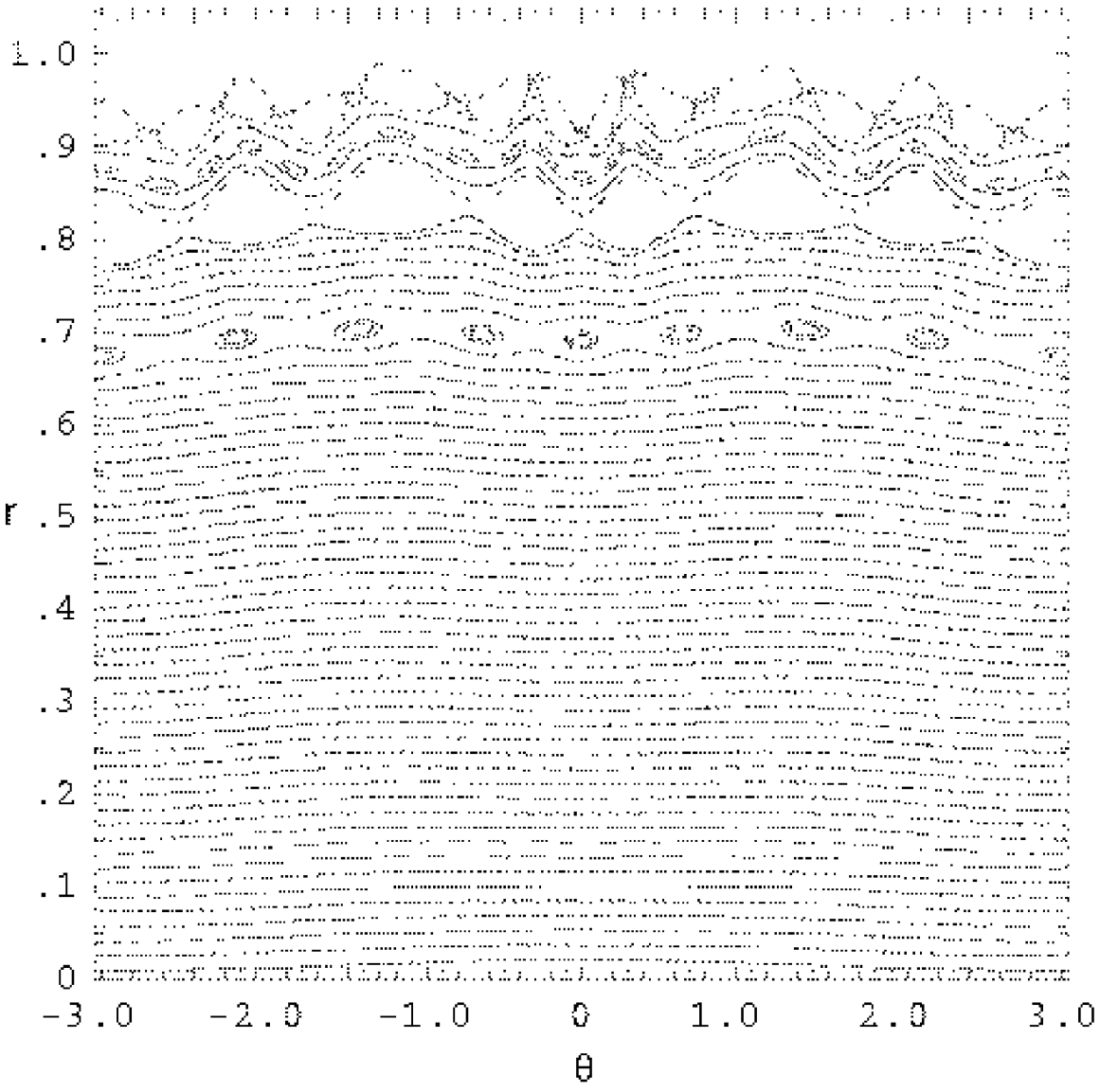

Figure 4: PIES free boundary calculation for the B_{err} targeted NESVD surface current solution. Note the large islands near edge. The next figure shows the positive effects of targeting X_{err} to remove these islands.

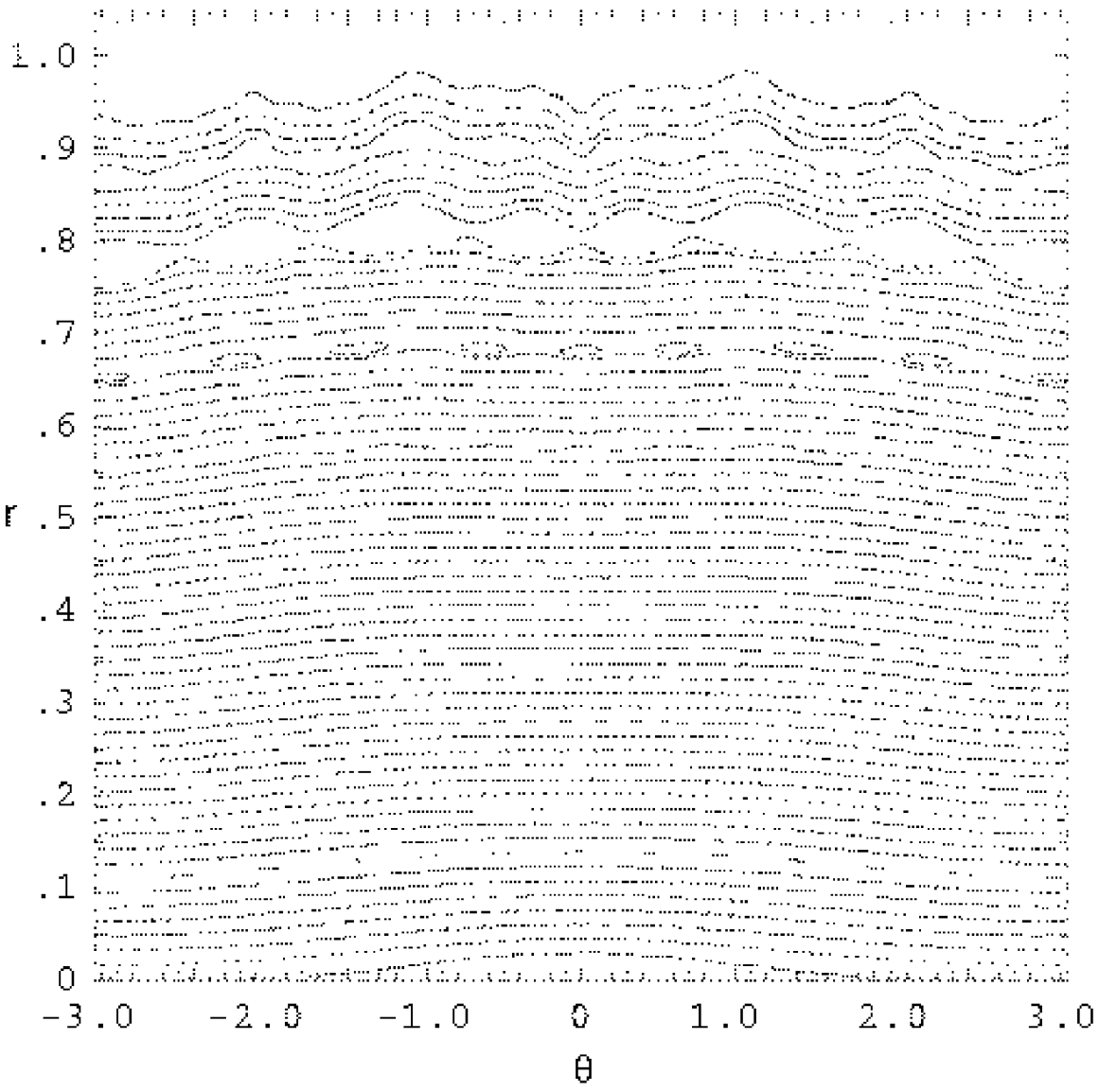

Figure 5: PIES free boundary calculation for the X_{err} targeted NESVD surface current solution. The large islands near the edge (previous figure) have been suppressed by X_{err} targeting.

The steps in this exercise were:

1. Run Xerror and Berror-targeted NESVD on d1826 surface for Li383 plasma to produce two current potentials. Calculate all errors (X and B) and Jmax etc.

2. Cut n ($6 \leq n \leq 20$) uniform coils per period (fixed step in current potential), and for each coilset calculate all errors (X and B) by using post-processor code B2xpp.

3. Use Berror+Jmax-targeted GA to cut n ($8 \leq n \leq 14$) coils per period with variable currents and non-uniform (variable step in current potential) coils. GA uses svd to choose best currents within GA to reduce combination of Berror and Jmax.

4. Make GA runs with different weights on Berr and Jmax (and soon Xerr) targets to reduce Jmax below 20 kA while keeping Berr low.

Note that a capability to target Xerr along with Berr and Jmax within GA has been implemented and is currently being benchmarked. It will be used when available.

Li383	*Xerr-Targeted-NESVD*		*Berr-Targeted-NESVD*	
Coils/period	Low Jmax	High Jmax	Low Jmax	High Jmax
8	19.75	26.2	15.66	21.7
Xerr	6.81E-04	8.78E-04	1.84E-03	1.56E-03
Xerr Max	2.55E-03	2.75E-03	5.20E-03	4.50E-03
Berr	8.99E-03	7.90E-03	8.74E-03	7.58E-03
Berr Max	4.15E-02	4.42E-02	3.79E-02	3.92E-02
Comments	*Promising*	*J too high*	*Bad Surfaces*	*J,X,B all High*
	Low Xerr, high Berr		*High Xerr & Berr*	
Status	*PIES-3-in progress*	*Don't run PIES*	*PIES-1-done*	*Don't run PIES*
14	18.2	33.45	16.25	22.23
Xerr	4.90E-04	1.03E-03	1.21E-03	1.12E-03
Xerr Max	1.55E-03	2.76E-03	3.74E-03	3.60E-03
Berr	9.11E-03	6.23E-03	7.90E-03	5.55E-03
Berr Max	4.23E-02	2.94E-02	3.82E-02	3.33E-02
Comments	*Best Xerr, high Berr*	*J too high*	*Xerr High, J low*	*Good Surf?*
	Too many coils?		*Berr not low*	*J high, B lowest*
Status	*Try PIES*	*Don't run PIES*	*Try PIES ?*	*PIES-2-done?*

1) All cases are with combinations of Berr & Jmax targeted in GA

Table 1

2) For Surface Current: Xerr = 1.55E-4 for Xerr targeted and 9.45E-4 for Berr targeted NESVD

Li383 High Beta GA Coils		Ratios of Errors to base case				Table 2	Actual Errors made by GA coils				Low
Case	Coils	XR	MXR	BR	BXR	COMMENTS	<|Xerr|>	Max |Xerr|	<|Berr|>	Max |Berr|	Jmax
Base: d1826.12.113.	60	1	1	1	1	Base Case	1.55E-04	9.49E-04	5.69E-03	2.89E-02	
XB -GA = X err targeted NESVD & B err targeted GA Coils											
ga.d1826.12.113.60.7.1.	14	6.62	2.90	1.09	1.02	*High Jmax*	1.03E-03	2.76E-03	6.23E-03	2.94E-02	33.45
ga.d1826.12.113.60.6.1.	12	5.91	3.45	1.17	1.17	*Do NOT*	9.16E-04	3.27E-03	6.63E-03	3.38E-02	24.53
ga.d1826.12.113.60.5.1.	10	6.14	3.56	1.19	1.29	*Run PIES*	9.51E-04	3.38E-03	6.78E-03	3.74E-02	24.9
ga.d1826.12.113.60.4.1.	8	5.67	2.90	1.39	1.53	*High Jmax*	8.78E-04	2.75E-03	7.90E-03	4.42E-02	26.2
XBJ -GA = X err targeted NESVD & B err+ J max targeted GA Coils											
ga.d1826.12.113.60.7.9.	14	3.16	1.63	1.60	1.45	*Low Jmax*	4.90E-04	1.55E-03	9.12E-03	4.19E-02	18.2
ga.d1826.12.113.60.6.9.	12	6.96	3.69	1.81	1.67	*Run PIES*	1.08E-03	3.50E-03	1.03E-02	4.82E-02	16.59
ga.d1826.12.113.60.5.9.	10	6.96	4.08	1.92	1.76	*On These*	1.08E-03	3.87E-03	1.09E-02	5.10E-02	15.6
ga.d1826.12.113.60.4.7.	8	4.39	2.69	1.58	1.44	*PIES-3 ???*	6.81E-04	2.55E-03	8.99E-03	4.15E-02	19.75
BB -GA = B err targeted NESVD & B err targeted GA Coils											
ga.d1826.11.126.60.7.1.	14	7.24	3.79	0.98	1.15	*PIES-2 good*	1.12E-03	3.60E-03	5.55E-03	3.33E-02	22.23
ga.d1826.11.126.60.6.1.	12	8.77	4.58	1.01	1.18	*Surfaces*	1.36E-03	4.35E-03	5.72E-03	3.40E-02	22.37
ga.d1826.11.126.60.5.1.	10	11.07	5.55	1.09	1.25	*But Jmax is*	1.72E-03	5.27E-03	6.18E-03	3.62E-02	22.71
ga.d1826.11.126.60.4.1.	8	10.09	4.74	1.33	1.36	*Too High*	1.56E-03	4.50E-03	7.58E-03	3.92E-02	21.70
BBJ -GA = B err targeted NESVD & B err+ J max targeted GA Coils											
ga.d1826.11.126.60.7.9.	14	7.84	3.94	1.39	1.32	*Low Jmax*	1.21E-03	3.74E-03	7.90E-03	3.82E-02	16.25
ga.d1826.11.126.60.6.9.	12	9.66	4.69	1.43	1.35	*Run PIES*	1.50E-03	4.45E-03	8.16E-03	3.89E-02	16.28
ga.d1826.11.126.60.5.9.	10	10.13	5.09	1.44	1.21	*On These*	1.57E-03	4.83E-03	8.19E-03	3.49E-02	16.1
ga.d1826.11.126.60.4.7.	8	11.88	5.48	1.54	1.31	*PIES-1 bad*	1.84E-03	5.20E-03	8.74E-03	3.79E-02	15.66

Li383 High Beta NESVD	Ratios of Errors to base case				Table 3	Actual Errors From uniform coils				
X-NES = Uniform Coils cut from Xerror targeted NESVD is Case 12										
Case	**Coils**	**XR**	**MXR**	**BR**	**BXR**	**COMMENTS**	**<|Xerr|>**	**Max |Xerr|**	**<|Berr|>**	**Max |Berr|**	**Jmax**
Base: d1826.12.113.	**60**	**1**	**1**	**1**	**1**	**Base Case**	**1.55E-04**	**9.49E-04**	**5.69E-03**	**2.89E-02**	**0.7605**
d1826.12.113.	20	4.31	1.99	1.10	1.02	These are	6.67E-04	1.89E-03	6.24E-03	2.95E-02	Note
d1826.12.113.	19	3.06	1.75	1.18	1.07	uniform	4.75E-04	1.66E-03	6.72E-03	3.09E-02	This is
d1826.12.113.	18	4.87	2.26	1.10	1.03	coils cut	7.55E-04	2.14E-03	6.26E-03	2.98E-02	in NESVD
d1826.12.113.	17	3.49	1.89	1.24	1.12	from nesvd	5.41E-04	1.79E-03	7.07E-03	3.23E-02	units
d1826.12.113.	16	6.51	3.15	1.17	1.06	Xerr-targeted	1.01E-03	2.99E-03	6.63E-03	3.06E-02	Surface
d1826.12.113.	15	3.75	2.05	1.37	1.12	Case 12	5.80E-04	1.95E-03	7.82E-03	3.24E-02	current
d1826.12.113.	14	4.50	2.27	1.37	1.29	which is	6.98E-04	2.15E-03	7.79E-03	3.72E-02	density
d1826.12.113.	13	5.10	2.47	1.56	1.21	used as the	7.91E-04	2.34E-03	8.88E-03	3.49E-02	All coils
d1826.12.113.	12	4.56	3.02	1.56	1.43	Base Case	7.06E-04	2.86E-03	8.88E-03	4.12E-02	have equal
d1826.12.113.	11	7.28	3.21	1.84	1.41	for GA runs	1.13E-03	3.05E-03	1.05E-02	4.08E-02	current
d1826.12.113.	10	4.73	2.75	1.80	1.55		7.33E-04	2.61E-03	1.03E-02	4.49E-02	GA gives
d1826.12.113.	9	12.78	6.32	2.38	1.76		1.98E-03	6.00E-03	1.35E-02	5.09E-02	current
d1826.12.113.	8	9.46	5.64	2.27	2.08		1.47E-03	5.35E-03	1.29E-02	6.01E-02	in coils
d1826.12.113.	7	16.24	8.01	3.33	2.37		2.52E-03	7.60E-03	1.89E-02	6.86E-02	A/cm^2
d1826.12.113.	6	19.21	9.76	3.08	2.92		2.98E-03	9.26E-03	1.75E-02	8.45E-02	
B-NES = Uniform Coils cut from Berror targeted NESVD is Case 11										
d1826.11.126.	**60**	**6.10**	**3.18**	**0.78**	**1.23**	**Berr-Nesvd**	**9.45E-04**	**3.02E-03**	**4.41E-03**	**3.57E-02**	**0.8214**
d1826.11.126.	20	6.75	3.64	0.95	1.23	These are	1.05E-03	3.45E-03	5.39E-03	3.55E-02	Note
d1826.11.126.	14	7.31	3.81	1.24	1.14	uniform	1.13E-03	3.61E-03	7.07E-03	3.29E-02	This is
d1826.11.126.	13	5.24	2.92	1.76	1.46	coils cut	8.11E-04	2.78E-03	1.00E-02	4.22E-02	in NESVD
d1826.11.126.	12	8.21	4.47	1.40	1.22	from nesvd	1.27E-03	4.24E-03	7.95E-03	3.53E-02	units
d1826.11.126.	11	7.33	4.20	2.15	1.78	Berr-targeted	1.13E-03	3.98E-03	1.22E-02	5.15E-02	All coils
d1826.11.126.	10	7.69	4.02	1.65	1.48	Case 11	1.19E-03	3.81E-03	9.37E-03	4.27E-02	have equal
d1826.11.126.	9	13.17	6.24	2.86	2.25		2.04E-03	5.92E-03	1.63E-02	6.51E-02	current
d1826.11.126.	8	8.89	4.30	2.14	2.04		1.38E-03	4.08E-03	1.22E-02	5.89E-02	

Plot 1: Jmax for GA Li383 d1826 from Xerr and Berr-targeted-NESVD
Within GA: Berr or Jmax is targeted for each coilset

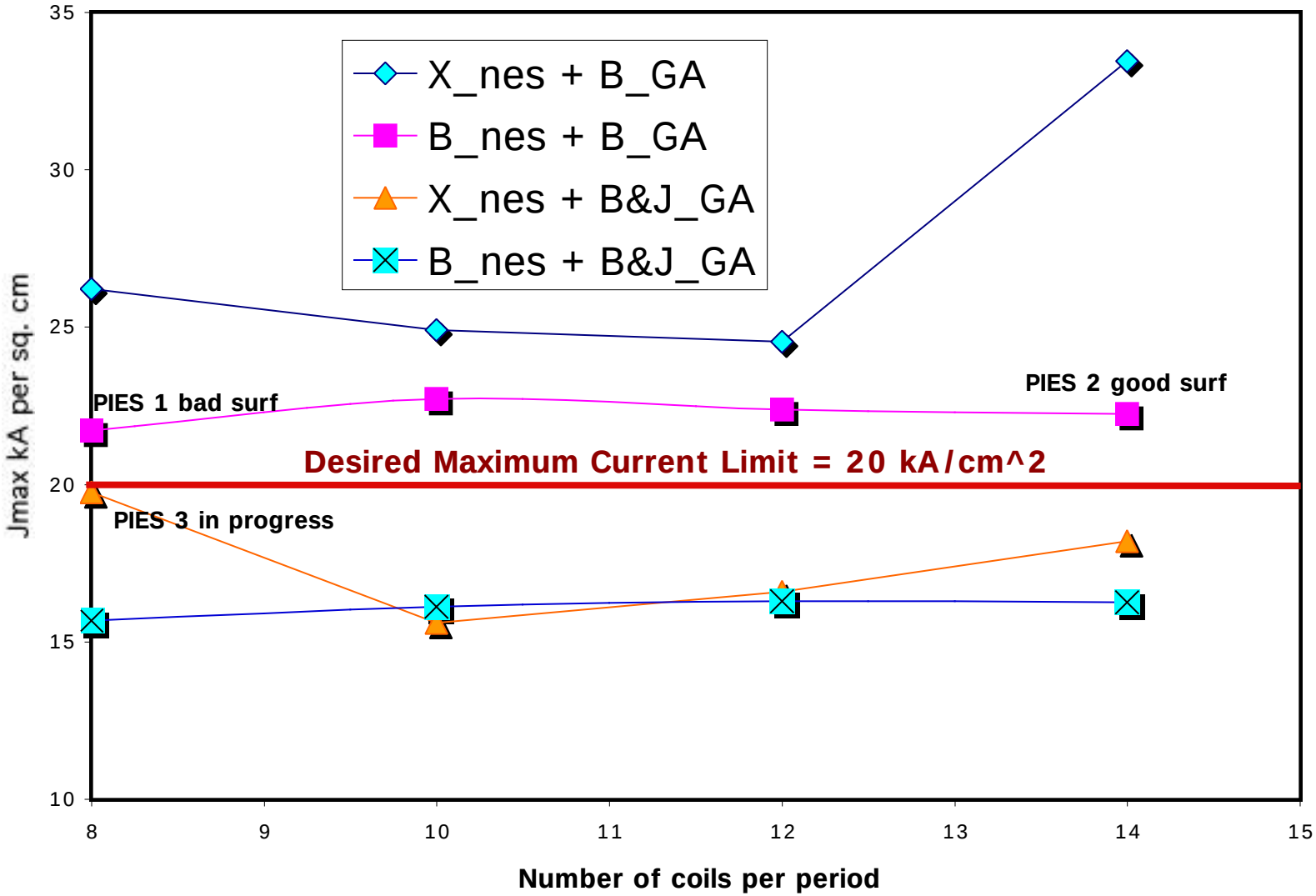

Plot 2: <|Xerr|> Normalized to <|Xerr|> for Xerr-Targeted-NESVD
Normalized <|Xerr|> for Berr-targeted surface current = 6.1

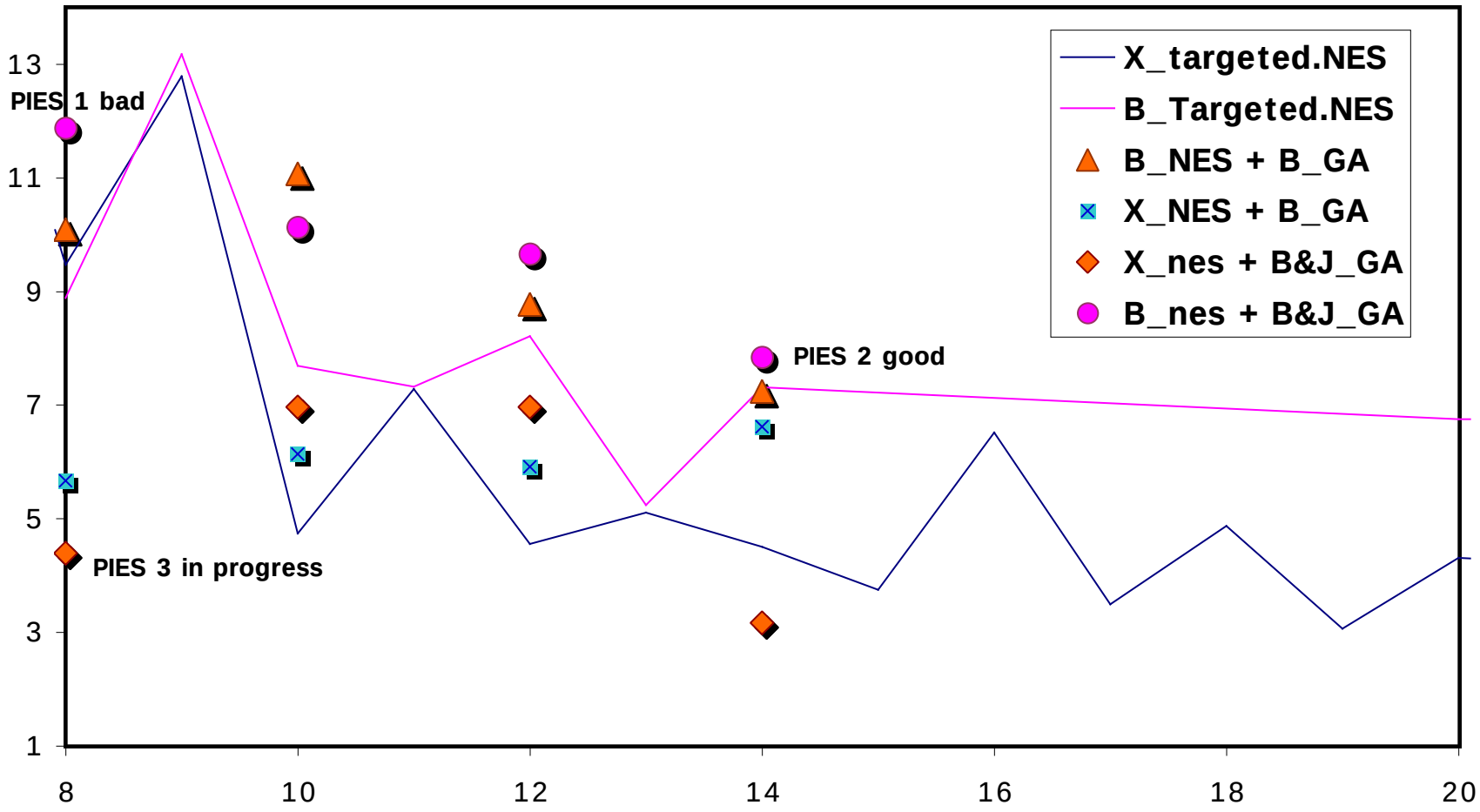

Plot 3: Max_Xerr Normalized to Max_Xerr for Xerr-Targeted-NESVD
Normalized Max_Xerr for Berr-targeted surface current = 3.18

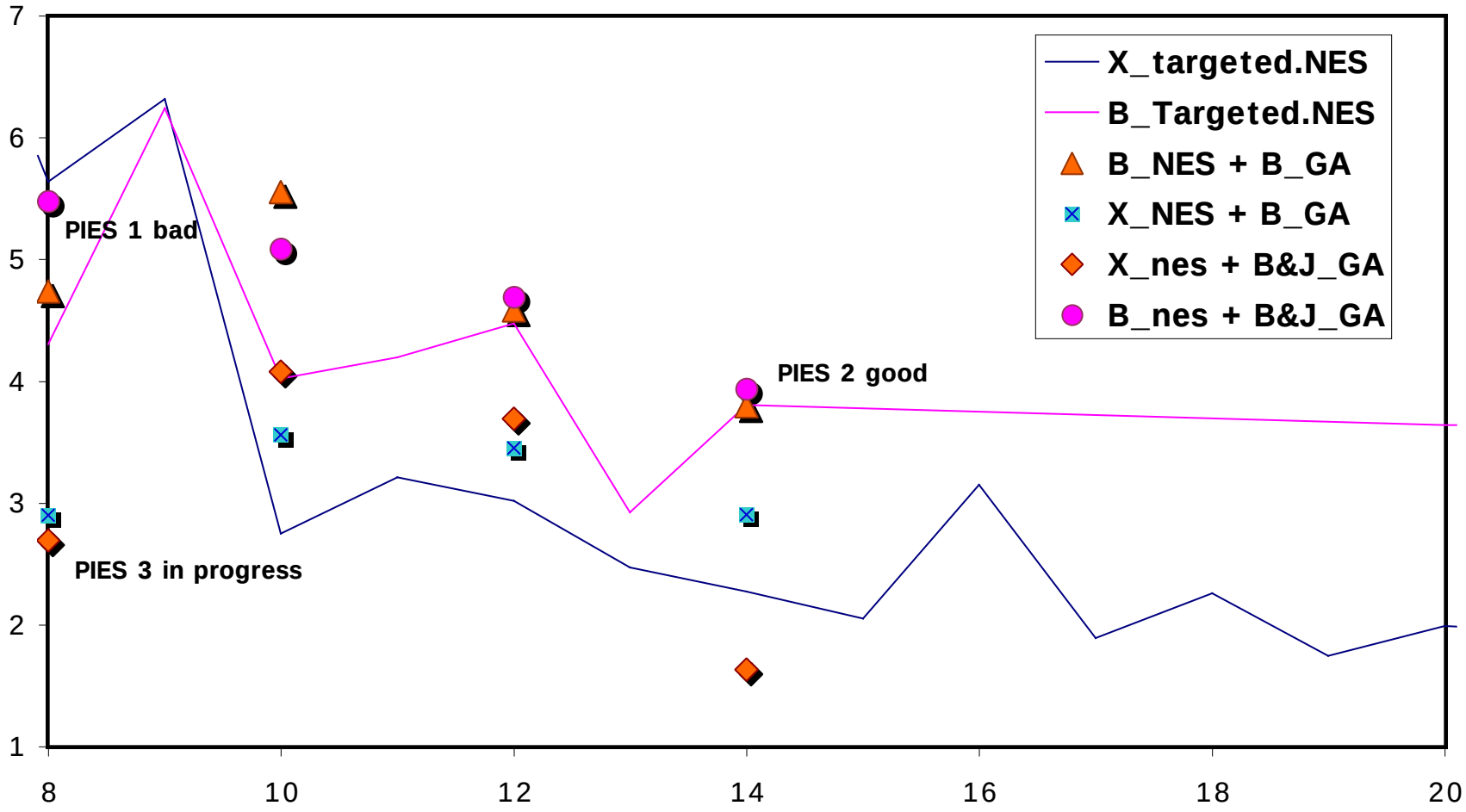

Plot 4: <|Berr|> Normalized to <|Berr|> for Xerr-Targeted-NESVD
Normalized <|Berr|> for Berr-targeted surface current = 0.78
Note that GA targets Berr and hence suppresses it

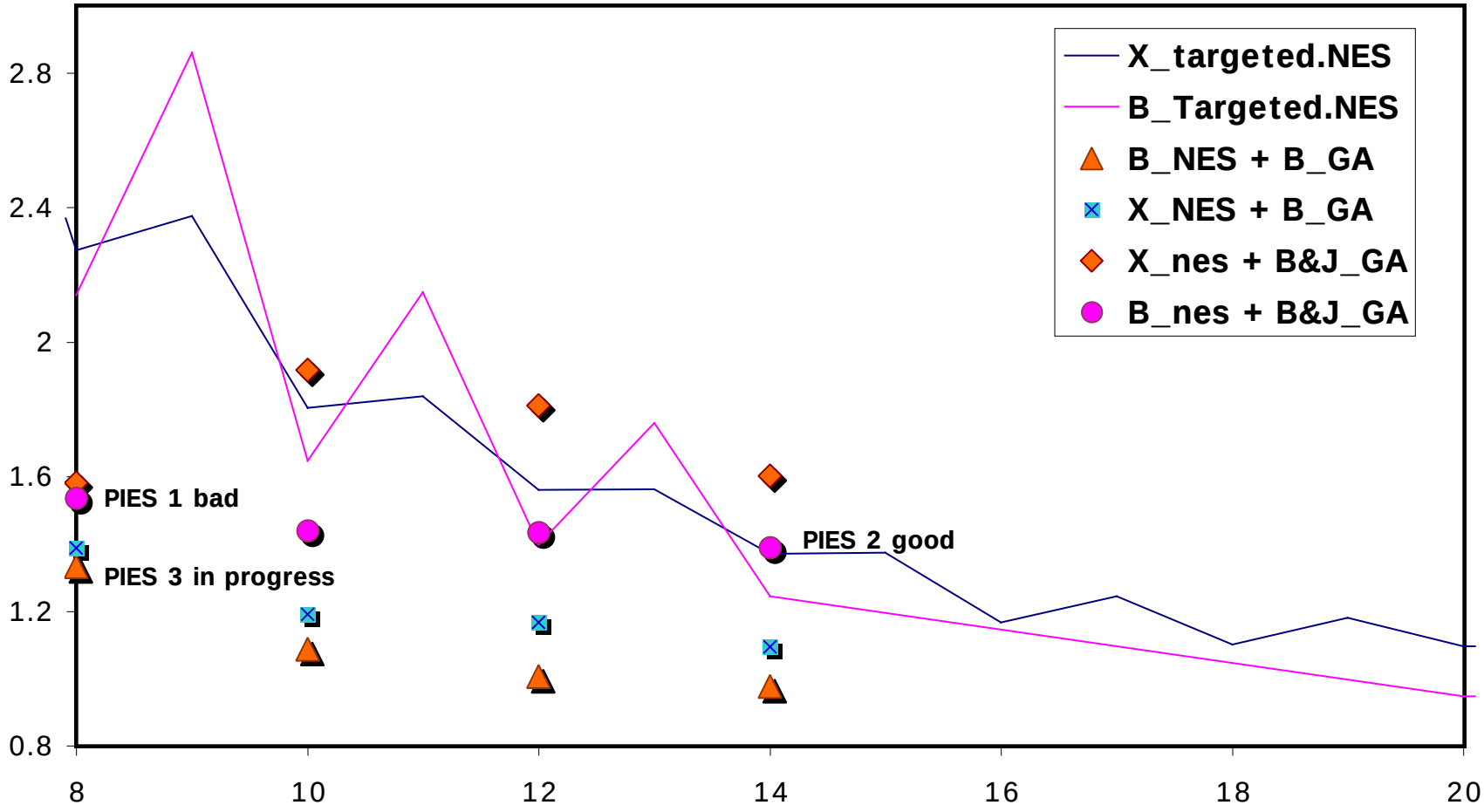

Number of coils per period (Uniform - no markers or GA - hollow markers)

Plot 5: Max_Berr Normalized to Max_Berr for Xerr-Targeted-NESVD
Normalized Max_Berr for Berr-targeted surface current = 3.18